

Motorized Mirror Controller with 3D Printed Parts

Dallen Petersen

A senior thesis submitted to the faculty of
Brigham Young University
in partial fulfillment of the requirements for the degree of
Bachelor of Science

Dallin Durfee and Richard Sandberg, Advisors

Department of Physics and Astronomy
Brigham Young University

Copyright © 2020 Dallen Petersen

All Rights Reserved

ABSTRACT

Motorized Mirror Controller with 3D Printed Parts

Dallen Petersen

Department of Physics and Astronomy, BYU

Bachelor of Science

A simple, low-cost, high-precision, motorized mirror controller is presented that was developed for use in a lensless imaging experiment. The goal was to achieve angular precision of better than 20 arc seconds while costing less than comparable commercial options. This is done using a standard kinematic mirror mount, high-pitch screws and stepper motors held together by 3D printed parts. The mount can be controlled by a python script on a Raspberry Pi or any other microcontroller connected to the motors. The mount can be quickly assembled for less than \$350 and achieves a large angular range (10 degrees). The accuracy is tested using a laser reflected off of a mirror controlled by the mount and projected onto the CCD of a webcam. The tested accuracy was 7.67 arc seconds with a standard deviation of 4.71 arc seconds.

Keywords: mirror, motorized, control, 3D printing, high-precision, interferometer

Contents

Table of Contents	iv
List of Figures	v
1 Introduction	1
1.1 Motivations	1
1.1.1 Interference Pattern Imaging	1
1.1.2 Further Applications	2
1.2 Prior Work at Brigham Young University	2
1.3 Overview	3
2 Methods	4
2.1 Mount Design	4
2.2 Cost	6
2.3 Testing Setup	7
2.4 Speed Tests	8
2.5 Image Stability	8
2.6 Backlash Correction	8
2.7 Single-Point Homing Accuracy Test	9
2.8 Multi-Point Homing Accuracy Test	9
2.9 Pointing Accuracy	10
3 Results and Conclusions	12
3.1 Speed Test	12
3.2 Homing accuracy	13
3.3 Pointing Accuracy	14
3.4 Conclusion	15
Bibliography	17

List of Figures

2.1	The mount when fully assembled. All of the white plastic is 3D printed. A spring holds the controller to the actuators while still allowing for free motion.	5
2.2	Diagram of how a stepper motor works. (M4RC0 2020)	6
2.3	Diagram of the test setup. The double lens system allows for the focus to be adjusted directly onto the detector and the adjustable mirror is controlled by the motorized mount. The beam is then reflected off of another mirror to increase the optical distance to the detector, allowing small mount motions to result in larger beam motions on the detector.	7
2.4	Motion of the beam as viewed by the detector in the homing accuracy test and how homing accuracy error is defined. We tested both the vertical and horizontal error together, as shown in the 3rd panel.	9
2.5	Motion of the beam as viewed by the detector in both the multi-point homing accuracy test and the pointing accuracy test. The red bar shows how error is defined for these tests.	11
3.1	The absolute error for the single-point homing accuracy test for 1000 test motions. The average error was 0.72 arc sec with a standard deviation of 0.47 arc sec.	13
3.2	The absolute error for the multi-point homing accuracy test for 1000 test motions. The average error was 5.27 arc sec with a standard deviation of 3.26 arc sec.	14

3.3	The absolute error for the pointing accuracy test using 1000 points. The average error is 7.67 arc sec with a standard deviation of 4.71 arc sec	15
-----	--	----

Chapter 1

Introduction

Conventional optical microscopes have limitations. High quality lenses are expensive to manufacture, they require the objective lens to be very close to the object and their theoretical resolution limit is the wavelength of visible light (Van Putten et al. 2011). We are currently developing a lensless interference pattern imaging technique that overcomes some of these limitations for optical microscopy.

1.1 Motivations

1.1.1 Interference Pattern Imaging

Interference pattern imaging improves upon conventional microscopes by no longer requiring expensive lenses, allowing objects to be imaged from a distance and decreasing the theoretical resolution limit to half the wavelength of the light used. We project interference patterns from an interferometer on to the object we are trying to image. We then vary the interference patterns using motorized mirror mounts and read out the intensity of the reflected light associated with each pattern. All of these intensity readings taken together give the Fourier transform of the image, which can

then be easily inverse transformed to complete the process. This method has potential applications in medicine, sonar, on-chip microscopy and x-ray radiography (Jackson & Durfee 2019).

Successful imaging with this method requires very precise mirror control so that the projected interference patterns are predictable. Commercial mounts achieve very good precision but lack angular range. In our case, angular range is important because it determines the size of an image that can be taken. Greater angular range on our motorized mirrors allows for larger images to be taken. Thor Labs offers a mount with 6 arc second precision and an angular range of 8 degrees. The mount and controller together cost \$2100 (ThorLabs 2020). Our goal was to develop a mount with precision of better than 20 arc sec, lower cost, and a higher angular range of 10 degrees.

1.1.2 Further Applications

Due to the low cost of these mounts, they could have further applications in undergraduate research and lab courses. Other low-cost mirror control options have been developed in the past, but not with the goal of high-precision (Gopalakrishnan & GÃijhr 2012). The mounts could be especially useful in precision laser spectroscopy, laser cooling and trapping, and biological imaging.

1.2 Prior Work at Brigham Young University

Jarom Jackson developed the mount designs for his thesis on interference pattern imaging (Jackson 2018). Other work on the imaging project was performed by Ben Whetten, on computational corrections for phase error, and Carter Day, on the effects of shadows on the resulting image. I tested the mount's limitations and worked on software-level performance improvements.

1.3 Overview

The mount can be assembled for less than \$350 and is accurate to around 7.67 arc sec, which is comparable to commercial mounts. It also has 10° of angular range, which is an improvement to commercial mounts. I outline the testing methods in Chapter 2 and provide specific results in Chapter 3.

Chapter 2

Methods

The primary goal in testing the mount was to determine how well the design would work for the imaging experiment discussed in Section 1.1.1. The secondary purpose was to characterize the limitations of the design more generally for any experimental application. The speed tests, discussed in Section 2.4, were done to determine how fast the motors can run without skipping steps. The three accuracy tests were the single-point homing accuracy, multi-point homing accuracy, and the pointing accuracy tests. The homing accuracy test, discussed in section 2.7, determined how accurately the mount can return to a position after moving away. Similarly, the multi-point homing accuracy test, discussed in Section 2.8, determined how well the mount can move between several different positions while the pointing accuracy test, discussed in Section 2.9, measures how well the mount can move to a desired position when its current position is known.

2.1 Mount Design

The mount parts are both easily obtained and relatively inexpensive. A picture of an assembled mount is found in Figure 2.1. We outfitted a standard 2 in. kinematic mirror mount with custom high-pitch screws. The actuators are controlled by stepper motors, which allow for high repeatability.

The motors are held together and connected to the mount with 3D printed parts (the white plastic in Figure 2.1), and a spring holds the motor controlling section to the kinematic mount.

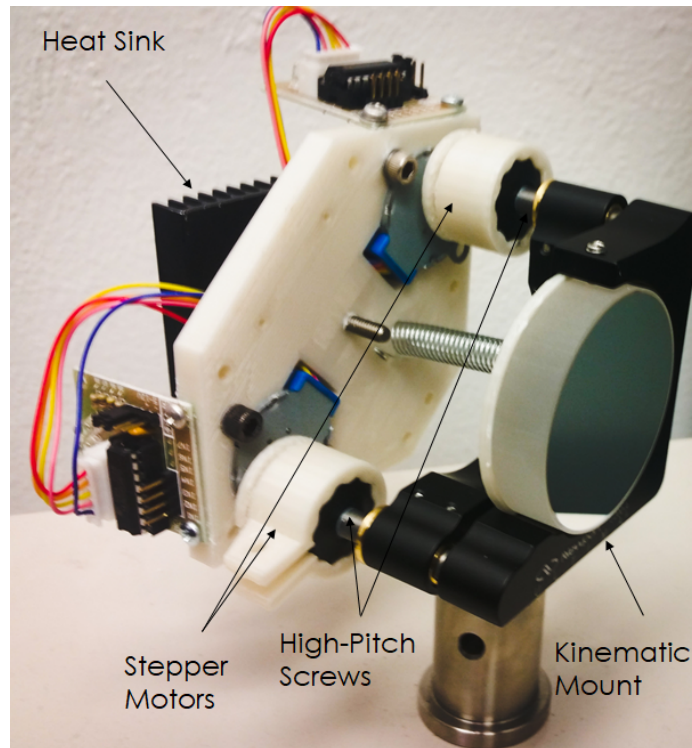


Figure 2.1 The mount when fully assembled. All of the white plastic is 3D printed. A spring holds the controller to the actuators while still allowing for free motion.

The high-pitch screws and the stepper motors are the keys to achieving high-precision and repeatability. The screws have 254 threads per inch, which allows small motor adjustments to translate into even smaller mount motions. A stepper motor, shown in Figure 2.2, consists of a series of electromagnetic coils that can be charged on or off independently (indicated as phases in the figure). Each configuration of charged and uncharged coils corresponds to a step. These discrete, repeatable steps makes it possible to move 100 steps in one direction and 100 steps back to finish with the motor mechanism in the original position.

We used Elegoo ULN2003 motors to turn the screws. The motors have 64 steps per rotation and were geared down by another factor of 64, resulting in 4096 steps per rotation. Combining these

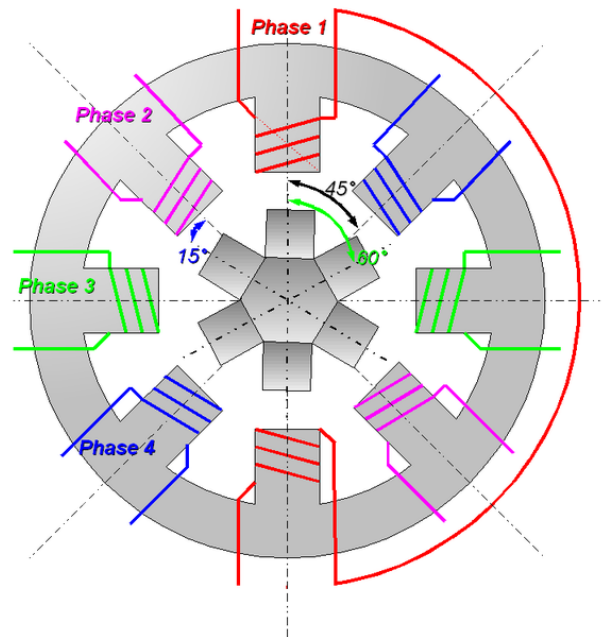


Figure 2.2 Diagram of how a stepper motor works. (M4RC0 2020)

effects with the high-pitch screws allows a single step to be incredibly small, only about 0.12 arc sec.

2.2 Cost

The total cost to assemble and control the mount was less than \$350. Below are approximate costs for each piece and the total is \$320:

- Newport 2 in. Kinematic Mirror Mount - \$140
- Newport high-pitch screws - \$120
- Elegoo motors - \$10
- Heat sink - \$5
- 3D printing filament - \$10

- Raspberry Pi 3 B+ - \$35

2.3 Testing Setup

To record the movements of the mount, we used a laser reflected off of a mirror controlled by the mount. As shown in Figure 2.3, two lenses were used to focus the laser down into a small spot on the detector, which was an HD Logitech webcam with the lens removed, so only the CCD was exposed. The location of the beam on the detector was determined by taking the average of the illuminated pixels.

Simple trig converts the pixels on the detector to angular movements of the mount. The motorized mirror is 0.78 meters from the detector (considering the reflection off the second mirror) and a single pixel was measured to be 3.67 microns on average using calipers to measure the CCD dimensions. Using the small angle approximation, this means that a single pixel spans:

$$\frac{3.67 * 10^{-6}}{0.78} = 4.71 * 10^{-5} \text{ rad} = .97 \text{ arc sec}$$

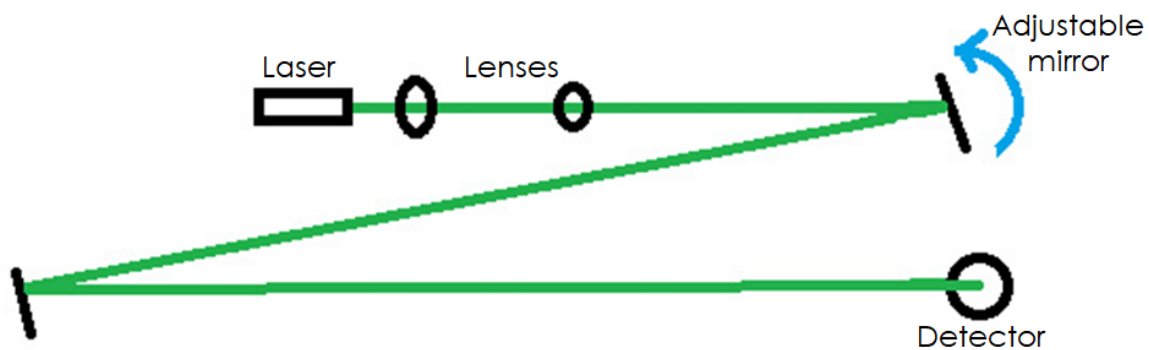


Figure 2.3 Diagram of the test setup. The double lens system allows for the focus to be adjusted directly onto the detector and the adjustable mirror is controlled by the motorized mount. The beam is then reflected off of another mirror to increase the optical distance to the detector, allowing small mount motions to result in larger beam motions on the detector.

2.4 Speed Tests

When the motors are run too fast or with too much torque, they will start to skip steps or stop moving entirely. The purpose of the speed test was to determine how fast the motors can run without skipping steps. To test this, the motors were run at progressively faster speeds by decreasing the wait time between steps. The location of the beam was recorded on the CCD and the average movement per step was measured at each speed. When the average speed dropped, it indicated the motors could not be reliably run that fast.

2.5 Image Stability

Because we are measuring such small motions, there was some inherent error in the measured location of the laser beam on the detector. To measure the baseline image stability, 1000 pictures were taken at 0.1 second intervals and the average location was calculated from each picture. We found there was an average deviation of 0.33 arc sec in the testing setup, indicating the limits of our error measurements. In most of our tests, the errors were much larger than this, so we can be confident in the results.

2.6 Backlash Correction

Gear backlash occurs when a motor with gearing switches directions. When the motor switches directions, one gear turns, but the small space between the gear teeth causes it to turn for a tiny bit before it catches the other gear. This effect is small in most applications but makes a significant difference when precision must be high. Without correction when moving the mount from one position to another and attempting to move straight back to the original position, backlash causes the mount to undershoot. Backlash can be corrected by moving slightly past the intended location

and then back the same number of steps, so the gear teeth are always pressed against each other on the same side. All of the tests were performed with this type of backlash correction.

2.7 Single-Point Homing Accuracy Test

The single-point homing accuracy test evaluates the ability of the mount to return consistently to a single position. We recorded initial position of the laser beam on the detector, moved both of the motors a full turn in one direction and a full turn back, then recording the final position of the beam. As shown in Figure 2.4, the distance between the original position and the final position is the error. This motion was repeated 1000 times.

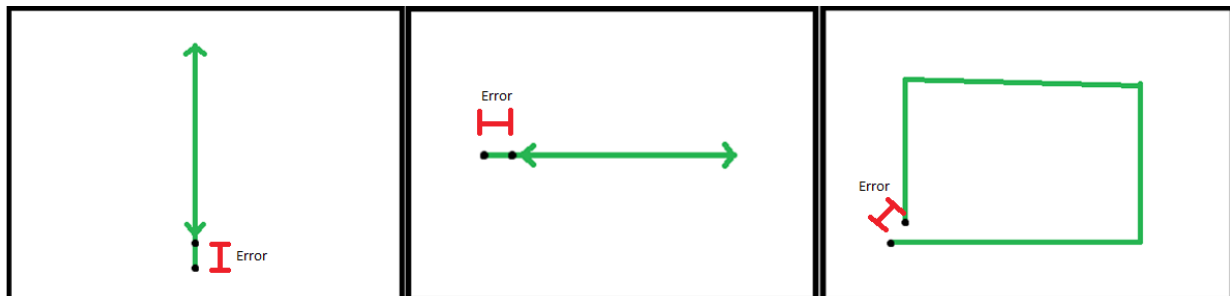


Figure 2.4 Motion of the beam as viewed by the detector in the homing accuracy test and how homing accuracy error is defined. We tested both the vertical and horizontal error together, as shown in the 3rd panel.

2.8 Multi-Point Homing Accuracy Test

The multi-point homing accuracy evaluates test the ability of the mount to move the beam consistently between multiple points. The original position becomes the origin for a coordinate system of steps. The mount moved the beam to 10 random locations on the detector. Each location was assigned a step coordinate which was used to determine how many steps in the y direction and the x direction the point is from the origin. Then, a random point from the first 10 was selected and the

current step coordinate (x_1, y_1) and the step coordinate of the selected point (x_2, y_2) were used to calculate how many steps to move $(x_2 - x_1, y_2 - y_1)$. After the motion, the distance in arc sec between the originally measured selected point (x_2, y_2) and the new measured location $(x_{\text{Real}}, y_{\text{Real}})$ was the error, just like the pointing accuracy test demonstrated in Figure 2.5.

2.9 Pointing Accuracy

The pointing accuracy test was designed to test how well the mount can be moved to a desired position from a known initial position by calculating the steps required to get there. This is especially important for our imaging experiment because we need the predicted mirror position to be very close to the actual mirror position for the projected interference patterns to be correct.

To test pointing accuracy, a random point on the detector is chosen in pixels $(x_{2\text{pixel}}, y_{2\text{pixel}})$ as the goal. The current position is measured $(x_{1\text{pixel}}, y_{1\text{pixel}})$ as the steps required to get to that point are calculated using the average step size for the motor $(x_{\text{Steps}}, y_{\text{Steps}})$. Once the mount has moved the calculated steps, the distance between the desired location and the actual location of the laser on the detector is the error, as shown in Figure 2.5. This motion was repeated 1000 times for each test.

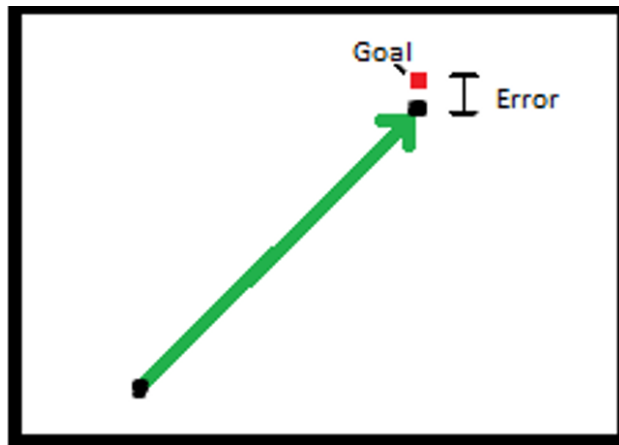


Figure 2.5 Motion of the beam as viewed by the detector in both the multi-point homing accuracy test and the pointing accuracy test. The red bar shows how error is defined for these tests.

Chapter 3

Results and Conclusions

As mentioned in Chapter 2, the primary goal in testing the mount was to determine how well the design would work for the imaging experiment discussed in section 1.1.1. The secondary purpose was to characterize the limitations of the design more generally for any experimental application. The speed test determined how fast the motors can run without sacrificing performance while the accuracy tests determined how accurately it can move in different scenarios.

3.1 Speed Test

The goal of the speed test was to determine how fast the motors can run without skipping steps. The average distance per step began to drop off below a wait period of 0.7 millisecond between steps and the motors completely stopped moving below 0.5 milliseconds. In order to have a healthy margin of safety, we ran the motors with a 1 millisecond delay for the rest of our tests. This corresponds to a scan rate of 468 steps per second, which works out to 8.75 seconds per rotation.

3.2 Homing accuracy

As shown in Figure 3.1, with backlash correction, the average absolute error was very low. After 1000 test points, the absolute error was only 0.72 arc sec with a standard deviation of 0.47 arc sec. Since the image stability is 0.33 arc sec (discussed in Section 2.5), the error is only slightly larger than our setup is capable of measuring. With the average step size being 0.12 arc sec (see Section 2.1), it is clear the mount can return to its original position within a few steps.

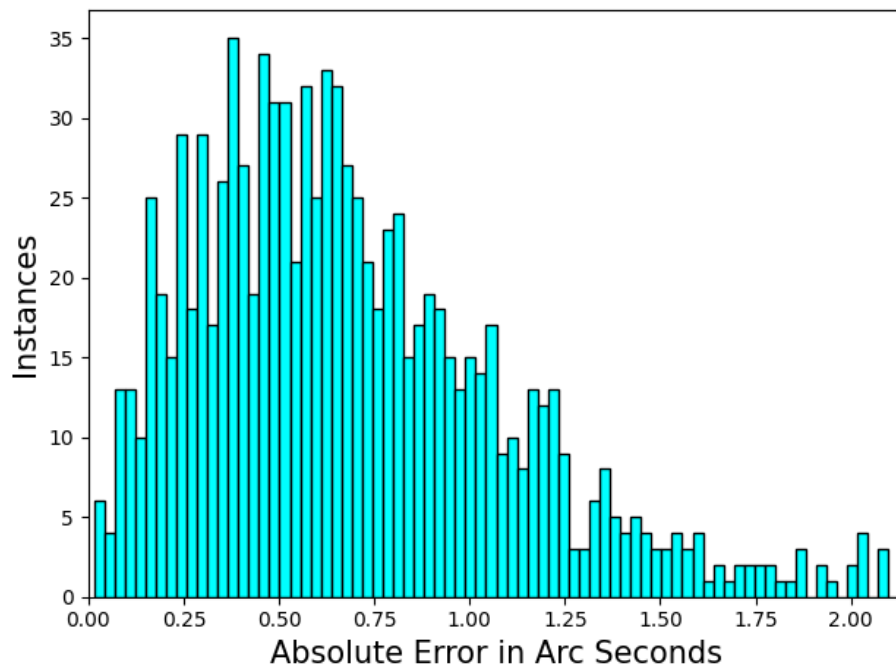


Figure 3.1 The absolute error for the single-point homing accuracy test for 1000 test motions. The average error was 0.72 arc sec with a standard deviation of 0.47 arc sec.

The results for the multi-point homing accuracy test, the absolute error was larger, but still very low. This is a more complicated test than the single-point accuracy test, naturally leading to larger expected error. In this case, the average absolute error was 5.27 arc sec with a standard deviation of 3.26. A few errors were as high as 15 arc sec, which is still acceptable for this test.

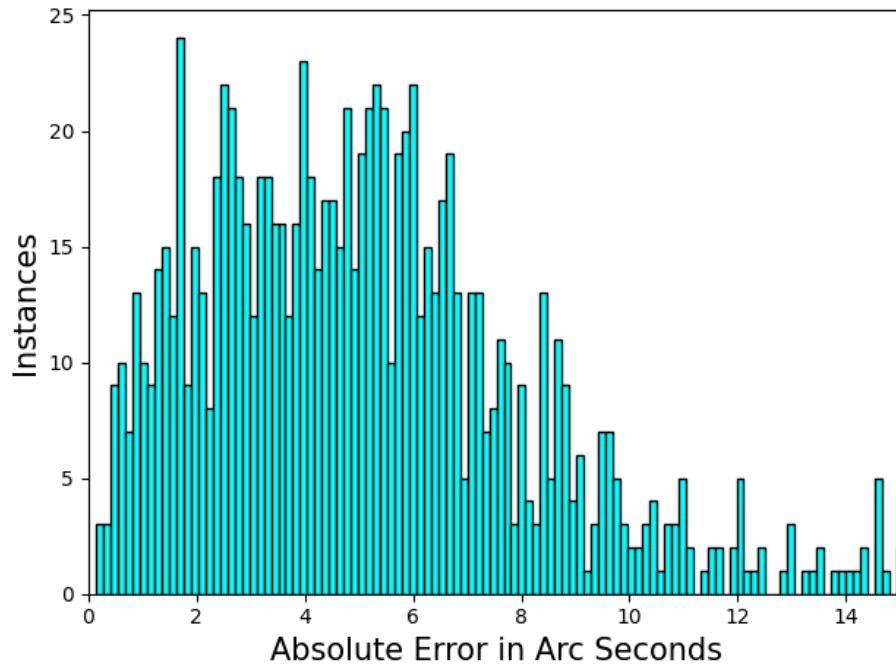


Figure 3.2 The absolute error for the multi-point homing accuracy test for 1000 test motions. The average error was 5.27 arc sec with a standard deviation of 3.26 arc sec.

3.3 Pointing Accuracy

The results of the pointing accuracy test, as shown in Figure 3.3, were especially impressive considering the difficulty of the problem. This test is the most reflective of the imaging experiment the mount was developed for (Section 1.1.1) and our goal was to get error below 20 arc sec. The average absolute error was only 7.67 arc sec with a standard deviation of 4.71 arc sec. Even given the relatively large standard deviation, very few points out of the 1000 tests had an absolute error slightly over 20 arc sec. This indicates that the accuracy is sufficient for the interference imaging experiment the mount was developed for.

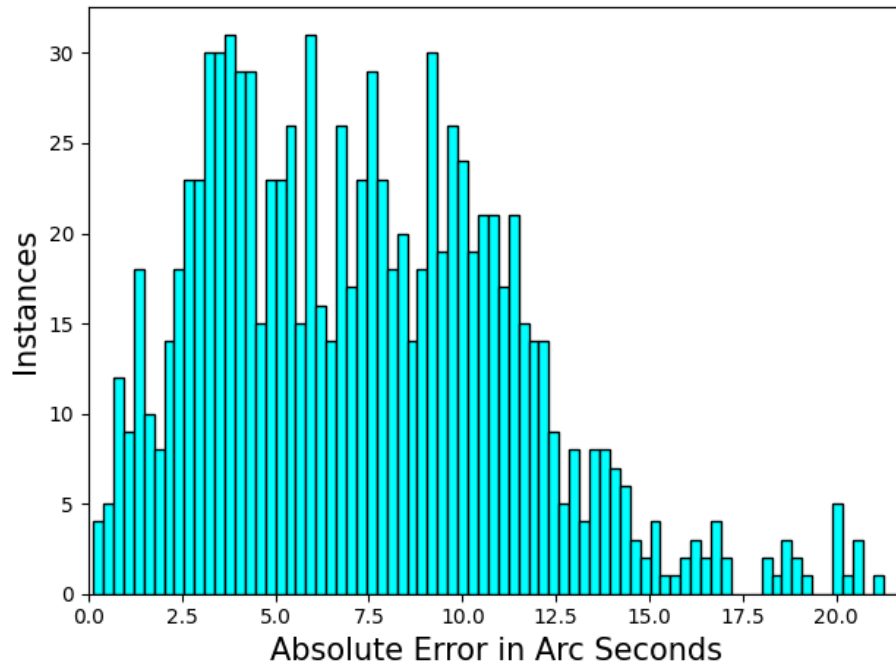


Figure 3.3 The absolute error for the pointing accuracy test using 1000 points. The average error is 7.67 arc sec with a standard deviation of 4.71 arc sec

3.4 Conclusion

The results, shown in Table 3.1, indicate the mount design is sufficient for use in our experiment. We were able to achieve an accuracy better than 20 arc seconds as well as an extra 2 degrees of angular range and a lower cost compared to the Thor Labs mount. While the accuracy is slightly worse than comparable commercial options, the extra angular range is more important for the imaging experiment the mounts were developed for (see Section 1.1.1). In other applications where the mount only needs to be accurate in a very small regime, the steps could be mapped to coordinates, like in the multi-point homing accuracy test. The only reason to do this over using a commercial mount, however, would be to save on the cost as the accuracy would be about the same and there would be no benefit from the increased angular range because the mapping would only be feasible in a small area where a detector could be used to record the locations.

Mount	Accuracy	Angular Range	Cost
Thor Labs	6 arc sec	8°	\$2100
Ours	7.46 arc sec	10°	\$350

Table 3.1 Comparison of our mount to a mount from Thor Labs.

Bibliography

Gopalakrishnan, M., & GÄijhr, M. 2012, arxiv

Jackson, J., & Durfee, D. 2019, Optics Express, 27, 14969

Jackson, J. S. 2018, PhD thesis, Brigham Young University, Provo, U.T.

M4RC0, W. C. 2020, Moteur pas Åã pas MRV

ThorLabs. 2020, Motorized Kinematic Mount

Van Putten, E. G., Akbulut, D., Bertolotti, J., Vos, W. L., Legendijk, A., & Mosk, A. P. 2011, Phys. Rev. Lett., 106, 193905